Fourier Transform Techniques for the Evaluation of the Thematic Mapper Line Spread Function

Walter H. Carnahan and *Guoping Zhou*
Physics Department, Indiana State University, Terre Haute, IN 47809

ABSTRACT: An endeavor was made to use Fourier Transform techniques to estimate the line spread function (LSF) of the Thematic Mapper (TM) from processed data. Data near the boundary of small fields from TM scenes were sampled, fitted to a theoretical curve, lowpass filtered, and then deconvolved to obtain the LSF. Lowpass filtering improved the truncation effect and eliminated the discontinuity at both ends of the data sequence. The selection of the cutoff frequency and the order of a lowpass filter is based on a newly defined criterion which tests the distortion of the processed edge by comparing it with the original edge. A parameter of the LSF, the equivalent width, is used to compare these LSF's deconvolved from sampled edge data with those evaluated by the derivative techniques. The calculated equivalent widths using the Fourier transform techniques for infrared bands are very close to TM design specifications.

INTRODUCTION

SPATIAL RESOLUTION is one of the most important specifications of the Landsat Thematic Mapper (TM) system. It has been demonstrated by Anuta *et al.* (1984) that land-use classification using TM data has a significant increase of classification accuracy in contrast with that using Landsat Multispectral Scanner (MSS) data. The spatial resolution of the TM system can be approximately characterized by the sensor's point spread function (PSF). The PSF describes how the imaging system, instrument, atmosphere, and processing responds to a point source of light. If the PSF is separable, i.e., if it can be written as a product of two orthogonal components, then the line spread functions (LSF) along these two directions can be treated as the components of the PSF at these directions (Zhou, 1984). The LSF describes how the imaging system responds to a line source. The nature of the scanning process implies that a natural line source would be oriented parallel to the satellite's path.

Schueler (1983) developed a methodology to characterize the TM LSF with prelaunched protoflight model optics and electronics measurements. An interesting result of the simulated TM LSF is that the side lobe ringing only occurred on one side of the main lobe. It is also noticeable that the ringing follows the scan motion rather than precedes it.

McGillem *et al.* (1983) used blurred edges from TM scenes to estimate the combined LSF of the TM system. The estimation was made by two methods in the spatial domain. The LSF was represented by a finite set of nonoverlapping rectangular basis functions which is a staircase approximation to the LSF. Another method was to utilize the scaled derivatives of smoothed data to estimate the LSF.

Zhou (1984) investigated the correlation of the atmosphere-sensor system LSF, calculated through deconvolution of sampled edge data, with particulate loading in the atmosphere. His study has shown that there is a certain degree of correlation between the LSF and the particulates. For a non-absorbing atmosphere, in general, the higher particulate concentration corresponds to wider equivalent width of the LSF. The implication of this result is that we can determine a TM sensor system LSF through study of measured data over a "clean air" area. The results for infrared bands reported in this paper give equivalent widths very close to the TM design specification.

THEORY

IMAGE MODEL

A remotely-sensed image, $g(x,y)$, can be regarded as the original scene, $f(x,y)$, convolved with system PSF, $h(x,y)$, and plus additive noise, $n(x,y)$: that is,

$$g(x,y) = f(x,y)*h(x,y) + n(x,y). \quad (1)$$

Our interest focuses on solving Equation 1 for the PSF $h(x,y)$. To this end we will average several measurements in order to estimate $h(x,y)$. We expect the estimates to contain contributions due to atmospheric scattering and image post-processing for registration and rectification as well as the conventional optical and instrumental contributions. While the

PHOTOGRAMMETRIC ENGINEERING AND REMOTE SENSING,
Vol. 52, No. 5, May 1986, pp. 639–648.

0099-1112/86/5205-639$02.25/0

instrumental terms are knowable, the effects of the atmosphere and to some extent those due to processing can be considered as random. If a set of remotely-sensed images is regarded as an ergodic random field, then $g(x,y)$, $h(x,y)$, and $n(x,y)$ can be treated as a sample from this random field. And if the number of such samples is large enough, then $E(h(x,y))$, the expectation of $h(x,y)$, which we evaluate by the mean, is an unbiased estimate of the system PSF. Assuming the actual image $f(x,y)$'s are time invariant and taking the expectation values of both sides of Equation 1, it follows that

$$E(g(x,y)) = f(x,y) * E(h(x,y)) + E(n(x,y)), \text{ or}$$

$$\hat{g}(x,y) = f(x,y) * \hat{h}(x,y) \quad (2)$$

where $\hat{g}(x,y) = E(g(x,y))$ and $\hat{h}(x,y) = E(h(x,y))$. Assuming that the noise is white with $E(n(x,y)) = 0$, the contribution of the second term on the right side vanishes. Theoretically, $\hat{h}(x,y)$ can be found through deconvolution of Equation 2; nevertheless, to collect a large number of images is practically unfeasible and unnecessary. The alternative is to assume the PSF is separable: that is,

$$h(x,y) = h(x)\,h(y). \quad (3)$$

Then its components can be estimated by the LSF of a bright line on a dark background along the y- or x-direction (Zhou, 1984).

Mathematically, the treatment for the LSF along the x- or the y-direction is the same, so only the LSF along the x-direction will be discussed.

Based on these assumptions, the two-dimensional model is simplified to one dimension: that is,

$$g(x) = f(x) * h(x) + n(x). \quad (4)$$

Instead of taking many samples of a scene at different times, many samples of the sensor's response to a particular scene element from an image can be extracted to form $g(x)$ where we assume that the scene element is extensive enough to be imaged by multiple scans. Because $E(n(x)) = 0$, the noise term $n(x)$ can be reduced through smoothing procedures, and the model becomes

$$\hat{g}(x) = f(x) * \hat{h}(x). \quad (5)$$

Here $\hat{g}(x)$ is the smoothed data, $f(x)$ is an ideal scene element, and $\hat{h}(x)$ is the estimated system LSF.

There are a number of ways to smooth the raw data $g(x)$. Smoothing can be done in the spatial domain through fitting the raw data with an appropriate theoretical curve, such as a trigonometric series. It can also be done through averaging $g(x)$ at equivalent distances with respect to the structure of the signal, i.e., each x-coordinate, and then low-pass filtering in the spatial frequency domain.

Scene Elements

According to McGillem *et al.* (1983), three scene elements can be used to study the LSF. They are

- an impulse represented by a narrow bridge or road along a line or a column of the data;
- a step represented by an edge along a line or a column of the data, such as the boundary between two fields; and
- a rectangular pulse represented by a sequence of two steps in opposite directions, such as a bright field between two uniform fields.

Theoretically, the impulse response at a certain direction is the system LSF along that direction. However, most linear features are too wide to be considered as an impulse. On the other hand, a feature, which is narrow enough, may not be identified from the background by the sensor system.

The third type of scene element is also difficult to be found in the real world and will not be discussed further in this paper.

The system response of a step is actually an edge spread function (ESF). It's derivative is the system LSF. That is,

$$\hat{h}(x) = d(\hat{g}(x))/dx. \quad (6)$$

Here $\hat{g}(x)$ is the smoothed edge data and $\hat{h}(x)$ is the estimated LSF.

Deconvolution of Fitted Edge Data

The LSF can be reconstructed through inverse filtering from Equation 2; that is,

$$\hat{h}(x) = F^{-1}\,(G(u)/F(u)) \quad (7)$$

where $G(u)$ and $F(u)$ are the Fourier transform of $g(x)$ and $f(x)$, respectively. The edge can be written as

$$f(x) = A + (B - A)u(x) \quad (8)$$

where $u(x)$ is the unit step function and A and B are the values on either side of the step. Then

$$F(u) = A\delta(u) + 1/i2\pi u(B - A). \quad (9)$$

The function $F(u)$ becomes infinite at $u = 0$ in both the real and imaginary parts, and division by this function is undefined. This is a result of the independence of the calculated LSF to a shift in the average value of $f(x)$. We utilize this independence when we normalize the calculated LSF.

For a continuous signal, the main difficulty involved in evaluating Equation 7 occurs when $F(u)$ equals zero. Gonzalez and Wintz (1977) point out that if the zeroes of $F(u)$ are located at a few known points in the frequency axis, they generally can be neglected when computing $F(u)$ without noticeably affecting the result.

For a discrete signal, however, the problem becomes more complicated because of the distortion of $G(u)$ due to aliasing and truncating effects on the data. Theoretically, aliasing is inevitable in obtaining the Fourier spectrum of a non-bandlimited sampled function. The main distortion of the Fourier transform of $\hat{h}(x)$, $H(u)$, results from the distorted high-frequency terms of $G(u)$. This is because the fitted data, $\hat{g}(x)$, are actually treated as a periodic function with period T, the length of raw data, when the discrete Fourier Transform is employed. Due to the truncating effect, there is a discontinuity between each two periods, and these discontinuous edges contain very high-frequency terms. Therefore, $H(u)$ does not approach zero at the high-frequency terms as expected.

To solve this problem we choose to use a lowpass filter (LPF) to filter out the fictitious high-frequency terms. The filtering process should be able to conserve the fitted edge of g(x) as far as possible. A criterion is introduced to optimally select the cutoff frequency and the order of a LPF. A similar technique was suggested by Gennery (1973).

For convenience, the hats of $\hat{g}(x)$ and $\hat{h}(x)$ will be dropped in the later discussion, so that $g(x)$ will refer to the smoothed edge data while $h(x)$ will refer to the estimated LSF.

Equivalent Width of an LSF

The LSF can be quantitatively characterized by an equivalent width which is defined as (McGillem *et al.*, 1983)

$$W = \int h(x)dx/h_{\max} \tag{10}$$

In the discrete case, the integral can be replaced by summation; thus,

$$W = \sum_{m=0}^{N-1} h(m\Delta x)/h_{\max}. \tag{11}$$

The geometric meaning of W is the width of a rectangle which has a height $h_{\max}$ and an area equal to the area between the LSF curve and x-axis. Obviously, the narrower W is, the less image degradation occurs, and the spatial resolution is narrower.

PROCEDURES

To apply this technique, we utilized available Thematic Mapper (TM) data. TM data (scene ID 40101-16025) were acquired 25 October 1982 for the Chicago metropolitan and surrounding area. To minimize the effects of atmospheric particulates, an area around Joliet (unwind from Chicago on that date) was searched for a field-edge oriented in an approximate North-South direction.

The sampled field edge was located immediately due south of a conservation forest and was regarded as an area with 'clear' atmosphere because of the contrast shown by features in the area. It was found that the edges selected had homogeneous features on either side. Eleven horizontally consecutive scan lines, which were nearly perpendicular to the edge, were selected to form a one-dimensional data sample. Each of the eleven lines utilized 17 of the 25 pixels in order to guarantee that there were eight pixels on either side of the edge.

To compress the two-dimensional sampled data of 11 lines with 25 pixels per line, the sampled data were fitted to a theoretical curve and then Tabatabai and Mitchells' (1984) approach was used to compute an edge location to subpixel accuracy.

After the edge location had been found, the "city block" distance (Rosenfeld and Kak, 1982) x from the edge was calculated for each data point. The distance was calculated in number of pixels with a step of a quarter pixel. Thus, the new data set had as its abscissa the distance of each data point to the edge (x = 0) and as its ordinate the grey tone at that point. For the points which have their $x>$o, the locations of these points are on the right side of the edge while, if $x<$o, the points are on the left of the edge.

The data points were fitted with an appropriate theoretical curve. A combination of a linear function and a Fourier series was chosen as a fitting function. Its analytical expression is

$$g(x) = ax + b + \sum_{k=1}^{n} \left(C_k \sin\frac{2\pi kx}{M} + D_k \cos\frac{2\pi kx}{M}\right) \tag{12}$$

where M is the length of data sequence measured in number of pixels (in this study, $M = 16$). This function has a good match to the edge data, and, by subtracting the linear trend of the signal the convergence of the Fourier series, was accelerated.

One of the most important problems in fitting data with the theoretical curve is how to determine the number of coefficients to be used in the fitting routine. Theoretically, it should be chosen as that value at which the magnitude of the envelope of the coefficients had decreased to that of the high frequency noise components (McGillem *et al.*, 1983). The problem is that the spectrum of the system noise is unknown; therefore, the choice of the number of coefficients was made subjectively by the investigator.

The continuous function, $g(x)$, was sampled to produce a sequence for the FFT. The fitted data sequence contains a discontinuity at both ends, which should be removed by lowpass filtering as discussed in the preceeding section. These discontinuities we refer to as spurious edges. We choose a Butterworth filter to remove these edges because

such a filter could be adjusted to solve the problem we discuss below, and, with a judicious choice of the parameters, it would not introduce any ringing. The main problems associated with the filtering process are how to determine the parameters of a Butterworth LPF and how to evaluate the filtered results. In the determination of the criterion, two facts were kept in mind. First, the spurious edges have a greater effective high-frequency term than actual edges do, and a properly selected cutoff frequency will reduce their influence on the frequency spectrum of $g(x)$. Secondly, total separation of the spectrum of a real edge from that of the fictitious edges is impossible. Generally, higher-order Butterworth LPF's rapidly attenuate the high-frequency terms which are greater than the cutoff frequency, D_o. On the other hand, the rapidly descending property of the abrupt transition will produce a ringing effect in the spatial domain. The experiments conducted in this study suggest that the second- and third-order Butterworth filters compromise these two aspects better than the others.

A criterion was established on the basis of comparing the real edge portions of $g(x)$ and $g'(x)$, which is the filtered $g(x)$. The attempt was made to use as small a cutoff frequency as possible, while limiting the distortion of the real edge portion of $g(x)$.

The form of the Butterworth LPF (Hanning, 1977) we used is given below.

$$L(u) = 1/(1 + (D/u)^{2N}) \tag{13}$$

where $L(u)$ is the LPF with D, the cut-off frequency, and N is the order of the filter. Then, the processed data are

$$g'(x) = F^{-1}(G(u)\,L(u)). \tag{14}$$

Here $G(u)$ is the Fourier transform of $g(x)$. The effectiveness of the filter can be tested by the χ^2-error criterion. The purpose of this is to provide a measure of the deviation of the fitted function from the original function. We will not use any probabilities associated with this measure.

The χ^2 error of $g(x)$ assumed to represent a probability distribution for the central 32 points can be calculated by

$$\chi^2 = \sum_{x=-4.0}^{3.75} \frac{(g'(x) - g(x))^2}{g(x)}. \tag{15}$$

Then, test if

$$\chi^2 < t \tag{16}$$

is satisfied: if not, repeat the same procedure until it is satisfied. Here t is a preset tolerance of deviation of the edge portion of $g'(x)$.

A program was written to recursively calculate the minimum D for each N for a given tolerance level. The values of N were limited to 6 or less to avoid strong ringing. Figure 1 shows several sets of paired N and D for three different χ^2 approximations of $g(x)$.

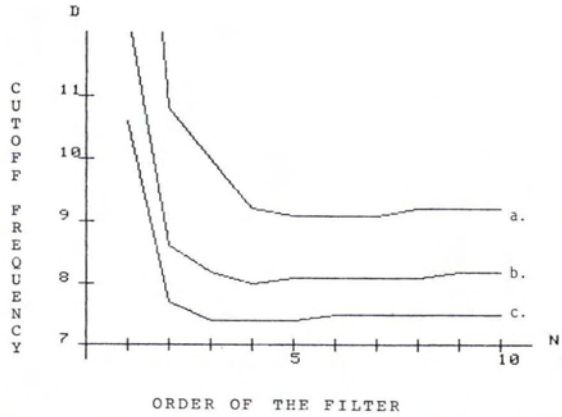

FIG. 1. The dependence of the cutoff frequency D on the order N for three X^2 error tolerances: (a) t = 0.01, (b) t = 0.05, and (c) t = 0.1.

The LSF $h(x)$ can be calculated with

$$h(x) = F^{-1}(F(g'(x))/F(f(x))). \tag{17}$$

The process can be briefly explained as follows:

First, the edge location of $g(x)$, denoted as X_e, and two brightness values A and B are found using Tabatabai and Mitchell's (1984) algorithm, $g(x)$ is processed by using an LPF with the parameters selected as above, and g'(x) is obtained: Set

$$\begin{aligned} f(x) &= B \text{ for } x > x_e \\ &= A \text{ for } x < x_e. \end{aligned} \tag{18}$$

Then perform the Fourier transform for g'(x) and f(x) and evaluate the ratio of their Fourier spectra. Finally, take the inverse Fourier transform, and the result is the required LSF, h(x). For the convenience of calculating LSF parameters for different bands, all maximum values of LSF's were normalized to unity. The delta function in Equation 8 was ignored, as it effects only the zero frequency part of the spectrum. This term, which determines the average value of h(x), is reset by the normalization.

Another difficulty related to calculation of the LSF with Fourier transform techniques is the wraparound error which creates some artifacts at each end of the truncation window. These artifacts can be reduced to tolerable levels by making the truncation window wide with respect to the important components of the signal and by filtering g(x) such that it has an equal amplitude at each end of the truncation window. Because the actual LSF's approach zero rapidly, it is reasonable that 32 to 40 of the 64 points can be taken to calculate the equivalent width of the LSF 's.

For comparison purposes, the LSF was also calculated from the derivative of the fitted edge and compared with the LSF calculated by the Fourier transform.

It was mentioned above that

$$h(x) = \frac{d(g(x))}{dx} \tag{19}$$

where $g(x)$ may be expressed in terms of a combination of a linear function and a Fourier series, as in Equation 12.

It is apparently simple to produce $d(g(x))/dx$ from Equation 12 immediately. However, the derivative of a good approximation is not necessarily a good approximation of the derivative of a function. This problem can be solved by multiplying the coefficients of the differentiated series with certain preassigned weight factors (McGillem *et al.*, 1983).

Thus,

$$\frac{\mathrm{d(g(x))}}{\mathrm{dx}} = a + \frac{2n}{\mathrm{M}} \sum_{k=1}^{n} \sin\frac{k\pi}{n} \left(C_k \cos\frac{2k\pi x}{M} - D_k \sin\frac{2k\pi x}{M} \right) \tag{20}$$

These same procedures were implemented on both the TM data and a simulated edge. The simulation data were produced by a convolution of an LSF with an ideal step. White noise, rectangular distributed with an amplitude of 20 percent of the step size, was added to the convolved step. The LSF used as input for the simulation had side lobes.

In order to observe how the number of coefficients in the fitting routine affects the shape of fitted curves and the corresponding LSF's, the edge data of Band 5 were trigonometrically fitted with 12, 16, and 20 coefficients (Figure 2).

The total number of coefficients used in the fitting routine may be determined by using the simulation edge. Start with a number of coefficients such as 10, implement with the same procedures as described in the preceding section, calculate the equivalent width for the obtained LSF, and compare the results with the LSF used as input to the simulation. If the deviation of the equivalent width of the output LSF calculated with Fourier technique from that of the simulated input LSF is greater than one-eighth pixel, increase the number of coefficients in the fitting routine and repeat the same process until the deviation is less than one-eighth pixel.

The derivative method has the advantages of simplicity and ease of calculation. Its disadvantage is that the derivative is very sensitive to the number of coefficients used in the fitting routine (Figure 2).

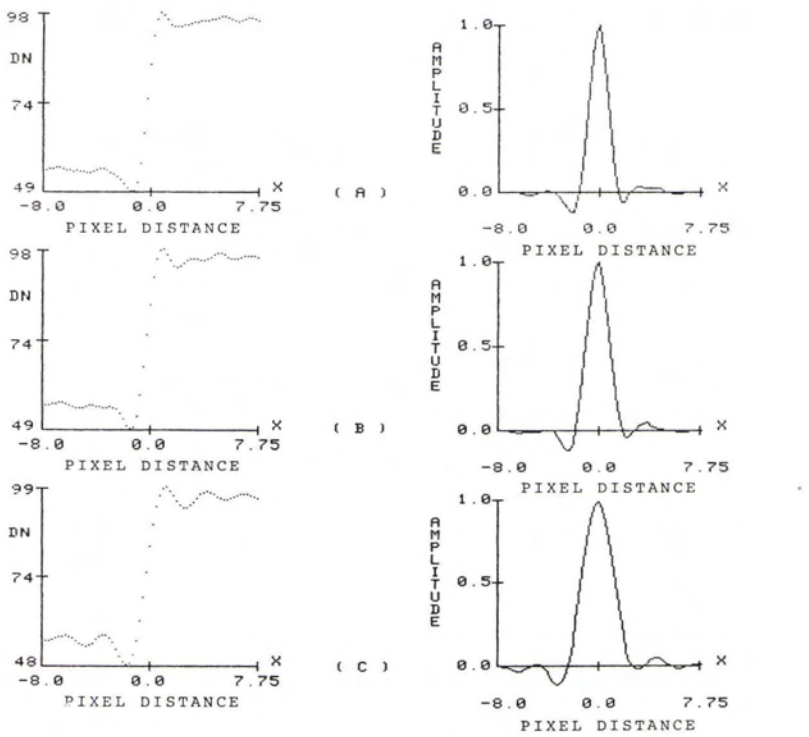

FIG. 2. Three sets of fitted curves of a field edge (left) and the corresponding LSF obtained by the derivative method (right). The distance is measured in pixels. (a) 12 coefficients are used in the fitting routine; (b) 16 coefficients are used in the fitting routine. (c) 20 coefficients are used in the fitting routine.

The calculated equivalent widths vary depending upon the number of coefficients. Another disadvantage this method has is that the derivative is sensitive to small variations. Thus, if the raw data have some abnormal points, the fitted curve will be controlled by these points, as will its derivative. In contrast with this method, the Fourier technique has its benefit of less control from a small number of abnormal raw data points because each point is associated with all the other points in the Fourier transform and the inverse Fourier transform (Figure 3).

There exists a formal equivalence between the derivative method and the transform method for the case we consider, i.e., when the signal, $f(x)$, is an ideal edge. The observation is based upon the fact that for nonzero values of the frequency the reciprocal of the transform of $f(x)$ is, ignoring the delta function for the reason mentioned above,

$$1/F(u) = 2\pi iu/(B - A), \; u \neq 0 \tag{21}$$

and, thus, Equation 17 becomes

$$h(x) = F^{-1}(G(u)/F(u)) = F^{-1}(CuG(u)) \tag{22}$$

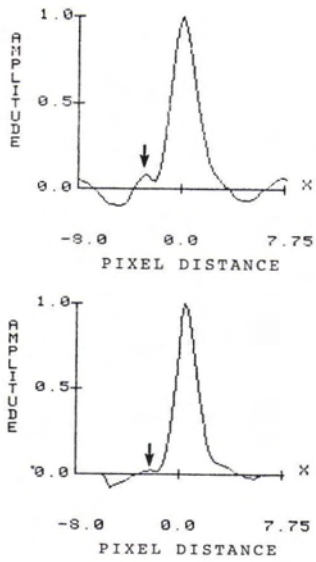

FIG. 3. Comparison of the LSF obtained by the derivative (a) and the Fourier techniques (b). Arrow indicates the local maximum of LSF which are controlled by some abnormal points in the derivative technique. Much less local control can be seen at the same location for the Fourier technique. The distance is measured in pixels.

where C is a constant. However, one may quickly show that

$$F^{-1}(u\,G(u)) = C'dg/dx. \tag{23}$$

An advantage of the transform method is that one may apply this technique to signals that are not ideal edges and, by dividing by the appropriate transform, obtain the LSF in a situation where there would not be an application of the method utilizing spatial derivatives.

Other differences between the two approaches can also be found through observation of Figure 3. First, the derivative method does not have an artifact involved at each end of the truncation window, while the Fourier method does. Second, the LSF derived from the Fourier method has a smaller width than that derived from the derivative method. This is particularly true when the chi-squared error is small. The question is: What is the best level of distortion tolerance for $g'(x)$?

It is evident that the best tolerance should correspond to that cutoff frequency at which $G(u)$ has a significant magnitude. If such a tolerance could be found, then the lowpass filtering with D and N calculated according to this tolerance would best retain the real edge and, at the same time, would smooth the fictitious edge. But it is difficult to determine such a threshold because the calculated discrete Fourier transform, $G(u)$, always contains the frequency spectrum of the fictitious edge. To separate its spectrum from that of a real edge requires a very long, finely sampled data sequence in order to guarantee high spectral and spatial resolution. In addition to some uncertainty of the Fourier transform of $g(x)$, the type of noise involved in the signal and its power spectrum is unknown; therefore, the determination of the number of fitting coefficients is somewhat subjective. These problems need further study.

RESULTS AND DISCUSSION

The LSF shape, as calculated from the simulated data, did not differ significantly from the LSF used as input in the simulation. The widths are compared in Table 1. As can be seen in Table 1, the transform method gives smaller widths than the derivative method. The widths as evaluated by the transform method are the same as the input widths to within 10 percent.

The effect of varying the number of coefficients (n) in Equation 12 is shown in Figure 2. Varying the number of coefficients in order to obtain one-eighth pixel accuracy for the transform method applied to the simulated data yielded a satisfactory fit with 20 coefficients. Because the LSF's calculated with the derivative method were too wide, they were not compared with the simulated input LSF in selecting the number of coefficients.

Figure 4 shows the scatter plots and the fitted smoothed curves for the data sets in six TM bands with the step of a quarter of a pixel. Because 20 total coefficients were used in the fitting routine, this makes 18 terms of a Fourier series plus a linear trend according to Equation 12.

The final result of the LSF's calculated by the derivative and Fourier transform methods for six TM bands are shown in Figures 5 and 6. Because the resampled data have one-eighth pixel accuracy, these LSF's will have one-eighth pixel, or ± 0.12 accuracy approximately. The maximum values for all LSF's were normalized to unity in order to calculate the equivalent width more conveniently. When the Fourier transform method was used, the data sets were tested with the χ^2 error criterion, and it was found that the optimal order of a Butterworth filter for a given threshold ($t = 0.1$) is two or three in most cases. For a certain amount of distortion of the central portion of a real edge, which is determined by a threshold t, the optimal order of a Butterworth filter should have a cutoff frequency as low as possible to smooth the fictitious edge to the greatest extent.

TABLE 1. A COMPARISON OF LSF WIDTHS FOR SIMULATED DATA. THE EQUIVALENT WIDTH IN PIXELS OF THE LSF AS DETERMINED BY SIMULATION. THE χ^2 FOR THE TRANSFORM METHOD WAS 0.5. THE ENTRIES ARE IN PIXELS. THE SECOND LINE GIVES THE VALUES FOUND WITHOUT ANY NOISE TERM.

	Input	Measured by Derivative Method	Measured by Transform Method
Equivalent Width	2.095	2.411	1.945
Equivalent Width (No noise)	2.0775	2.416	1.820

It is noticeable that the margin portions of the LSF's in Figures 5 and 6 are flattened purposely. It was discussed in the preceding section that the margin portions of the LSF's obtained using the Fourier technique are erroneous because of the wraparound error in applying the discrete convolution theorem. On the other hand, the emphasis of calculating the equivalent width is focused on the small neighborhood about the main lobe of the LSF. The side lobes of a LSF are expected to vanish rapidly and, thus, are unimportant. Therefore, ignoring these parts will not produce a significant error in the calculation of the equivalent width unless the amplitude of the side lobes is comparable with that of the main lobe. This was not a problem in the calculation of the TM LSF.

Figures 5 and 6 also show that the estimate of the LSF by using the derivative method is consistently wider than that obtained by using the Fourier transform method. The width reduction of an LSF derived by the derivative method, however, seems to

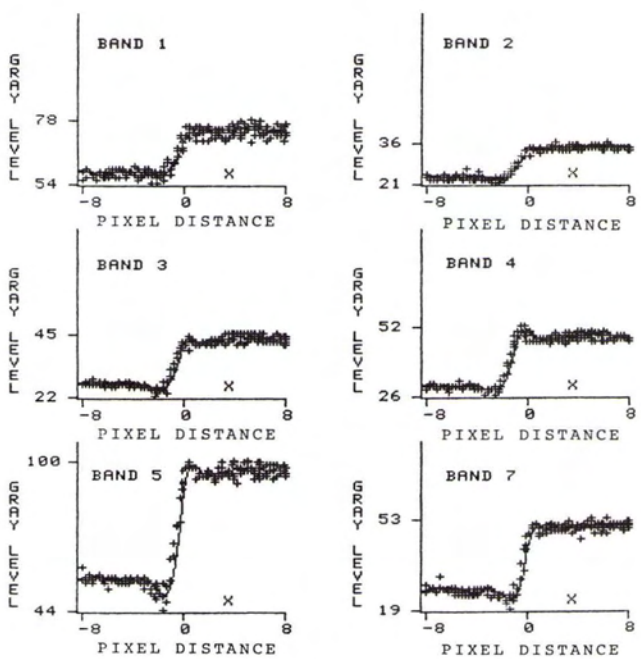

FIG. 4. Raw data and the fitted curves for the six TM bands. The distance is measured in pixels.

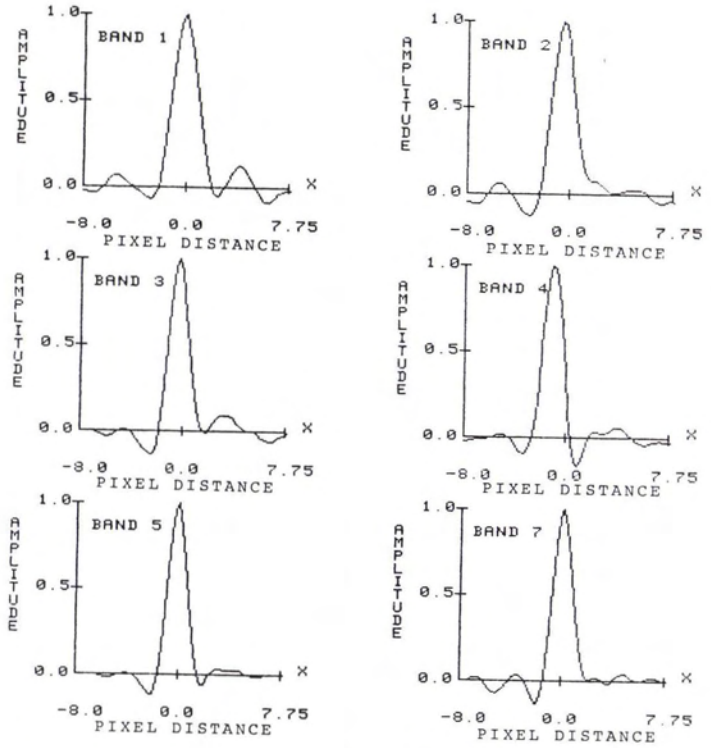

FIG. 5. The LSF calculated with the derivative method for six TM bands. The distance is measured in pixels.

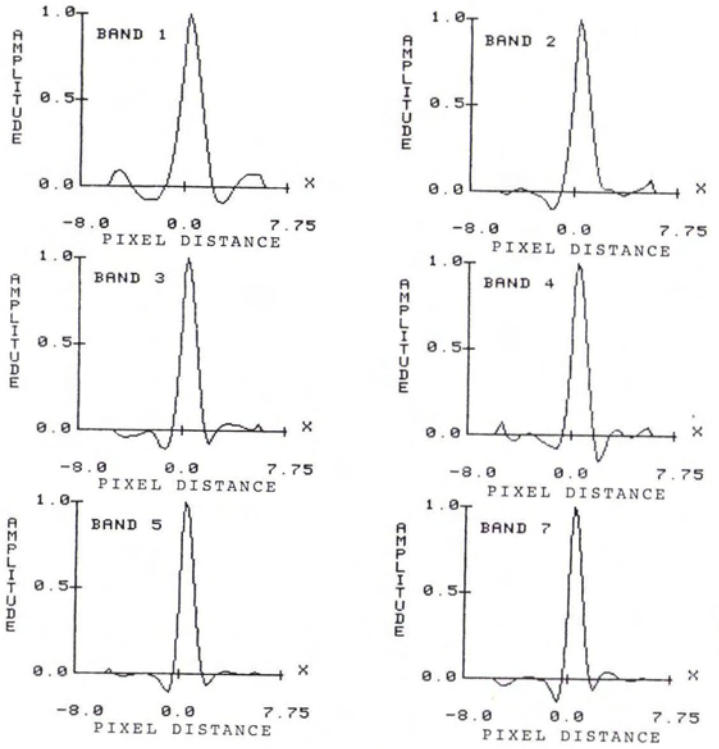

FIG. 6. The LSF calculated with the Fourier transform method for six TM bands. The distance is measured in pixels.

be rather rapid as the trigonometric terms increase in fitting the raw data (Figure 2). In contrast with this, the width reduction of the LSF's derived with the Fourier transform method is relatively insensitive to the increase in the coefficients in the fitting process. This may be a topic for future study.

Table 2 shows the widths evaluated for the "clear" edge mentioned above. These widths for the long wavelength bands 3 to 6 are surprisingly close to the prelaunch specifications. We may observe that widths for the transform method are uniformly smaller than those for the derivative method at both tolerance levels. Furthermore, all the widths (each row of the table) show a systematic decrease with increasing wavelength, particularly among the first three bands. We believe this is attributable to the inclusion of atmospheric scattering effects in these effective LSFs. Rayleigh scattering predicts a rapid decrease in the molecular scattering contribution to the LSF with increasing wavelength.

Markham (1984) has provided an evaluation of the TM LSF that combines the effects of the detector, optics, and electronics. For the detector LSF he used measured values. The optical and electronic LSF's were carefully modeled, and the three terms were convolved to give an overall LSF. Thus, his results do not include the atmospheric and post-processing effects. The corresponding widths are given in Table 3 along with those reported by McGillem *et al.* (1983).

TABLE 2. A COMPARISON OF LSF WIDTHS FOR TM BANDS. THE EQUIVALENT WIDTHS OF THE "CLEAR" FIELD EDGE AS SEEN IN SIX (EXCLUDING THE THERMAL BAND) OF THE TM BANDS, ARRANGED IN ORDER OF INCREASING WAVELENGTH. WD IS THE WIDTH CALCULATED WITH THE DERIVATIVE METHOD. WF.1 IS THE WIDTH CALCULATED WITH THE TRANSFORM METHOD WITH AN χ^2 TOLERANCE OF 0.1.

	Band 1	2	3	4	5	7
WD	2.24	1.90	1.59	1.44	1.54	1.61
WF	1.52	1.46	1.44	1.38	1.26	1.20
WF.1	1.68	1.39	1.15	1.06	1.05	0.96

TABLE 3. A COMPARISON OF LSF WIDTHS AS REPORTED BY OTHER INVESTIGATORS. THE ENTRIES ARE IN PIXELS. MARKHAM'S VALUES ARE TAKEN FROM HIS TABLE 9a USING THE PREFLIGHT VALUES (PF) WITH AN IFOV OF 42.5 MICRORADIANS FOR BANDS 1-4 AND AN IFOV OF 43.75 MICRORADIANS FOR BANDS 5,7. MCGILLEM'S VALUE REPRESENTS AN AVERAGE OF TWO EDGES TAKEN FROM THEIR TABLE 2.

Markham	Markham	McGillem *et al.* (1983)
Bands 1-4	Bands 5, 7	Band 4
1.213	1.185	1.45

CONCLUSION

This study is a new attempt to evaluate an LSF. The concept undertaken in this study is explicit and it is easy to fulfill. A particular endeavor was made to use Fourier techniques to achieve this goal. Because the Fourier technique has a more universal usage with other ground features than field edges, the research to explore its application is of great significance. For instance, if the third type of scene element (see second section) can be found in a scene, then the system LSF can be calculated through deconvolving a rectangular pulse even without lowpass filtering because, in this case, there is no discontinuity between two periods of fitted data. Furthermore, even if a "pulse" does not have equal levels on its both sides or, equivalently, a bright field between two non-uniform fields, the system LSF still can be obtained through deconvolving the "pulse' response (in a strict sense, it cannot be called a pulse because of inequality of the low levels on both sides) by lowpass filtering the raw data.

One of the most important problems in using Fourier techniques to calculate LSF is in how to evaluate the effects of lowpass filtering on raw data. Calculation of χ^2 error has been used in this study to test the effectiveness of the lowpass filtering. Another criterion was also mentioned in Zhou's paper (Zhou, 1984).

The equivalent widths calculated with the methods and techniques outlined in this work are very close to TM design specifications. Considering the possible one-eighth pixel resampling error and atmospheric effects, this is particularly true for bands 3 to 6 with a χ^2 tolerance level of 0.1.

ACKNOWLEDGMENTS

The authors wish to thank Paul Anuta, Clare McGillem, and Erik Malaret for generously sharing the results of their work with us. The Thematic Mapper data were obtained courtesy of LARS/Purdue University through a TM data quality analysis study which that laboratory is conducting for NASA under contract NAS 5-26859.

REFERENCES

Anuta, P. E., Luis A. Bartolucci, M. Ellen Dean, D. Fabian Lozano, Erick Malaret, Clare D. McGillem, Jose A. Valdes, and Carlos R. Valenzuela, 1984. Landsat-4 MSS and Thematic Mapper Data Quality and Information Content Analysis, *IEEE Transactions on Geoscience and Remote Sensing*, Vol. GE-22, No. 3, pp. 222–236.

Castleman, K. R., 1979. *Digital Image Processing*, Prentice-Hall, Inc., New York.

Gennery, D. B., 1973. Determination of Optical Transfer Function by Inspection of Frequency-Domain Plot, *Journal of the Optical Society of America*. Vol. 63, No. 12, pp. 1,571–1,577.

Gonzalez, R. C., and P. Wintz, 1977. *Digital Image Processing*, Addison-Wesley Publishing Company.

Hamming, R. W., 1977. *Digital Filters*, Prentice-Hall, Inc., New Jersey, p. 188.

Markham, B. L., 1984. *Characterization of Landsat Sensor's Spatial Response*, NASA/Goddard Space Flight Center, Greenbelt, Md.

McGillem, C. D., P. E. Anuta, E. Malaret, and K. B. Yu, 1983. Estimation of a Remote Sensing System Point Spread Function from Measured Imagery, *Proceedings of Machine Processing of Remotely Sensed Data*, Purdue University, Indiana, pp. 62–68.

Rosenfeld, A., and A. C. Kak, 1982. *Digital Picture Processing*, Academic Press, New York.

Schueler, C., 1983. Thermatic Mapper Protoflight Model Line Spread Function, Seventh International Symposium on Remote Sensing of Environment, ERIM, Ann Arbor, Michigan.

Tabatabai, A. J., and O. R. Mitchell, 1984. Edge Location to Subpixel Value in Digital Imagery, *IEEE Transactions on Pattern Analysis and Machine Intelligence*. Vol. PAMI-6, No. 2.

Zhou, G., 1984. *Evaluation of Atmospheric Particulate Blurring Effects through Analysis of the Line Spread Function of the Atmosphere-Sensor*, Master's Thesis. Indiana State University. Series I. Number 1483. p. vii + 64.

(Received 5 February 1985; revised and accepted 13 December 1985)
